

See discussions, stats, and author profiles for this publication at: <https://www.researchgate.net/publication/263510305>

# Genetic Encoding of Caged Cysteine and Caged Homocysteine in Bacterial and Mammalian Cells

ARTICLE *in* CHEMBIOCHEM · AUGUST 2014

Impact Factor: 3.09 · DOI: 10.1002/cbic.201400073

CITATIONS

7

READS

32

6 AUTHORS, INCLUDING:



[Rajendra Uprety](#)

Memorial Sloan-Kettering Cancer Center

12 PUBLICATIONS 191 CITATIONS

SEE PROFILE



[Subhas Samanta](#)

University of Pittsburgh

27 PUBLICATIONS 348 CITATIONS

SEE PROFILE



[Alexander Deiters](#)

University of Pittsburgh

135 PUBLICATIONS 4,977 CITATIONS

SEE PROFILE

# Genetic Encoding of Caged Cysteine and Caged Homocysteine in Bacterial and Mammalian Cells

Rajendra Uprety,<sup>[a]</sup> Ji Luo,<sup>[b]</sup> Jihe Liu,<sup>[b]</sup> Yuta Naro,<sup>[b]</sup> Subhas Samanta,<sup>[b]</sup> and Alexander Deiters<sup>\*[a, b]</sup>

We report the genetic incorporation of caged cysteine and caged homocysteine into proteins in bacterial and mammalian cells. The genetic code of these cells was expanded with an engineered pyrrolysine tRNA/tRNA synthetase pair that accepts both light-activatable amino acids as substrates. Incorporation was validated by reporter assays, western blots, and mass spectrometry, and differences in incorporation efficiency were explained by molecular modeling of synthetase–amino acid interactions. As a proof-of-principle application, the genetic replacement of an active-site cysteine residue with a caged

cysteine residue in *Renilla* luciferase led to a complete loss of enzyme activity; however, upon brief exposure to UV light, a >150-fold increase in enzymatic activity was observed, thus showcasing the applicability of the caged cysteine in live human cells. A simultaneously conducted genetic replacement with homocysteine yielded an enzyme with greatly reduced activity, thereby demonstrating the precise probing of a protein active site. These discoveries provide a new tool for the optochemical control of protein function in mammalian cells and expand the set of genetically encoded unnatural amino acids.

## Introduction


Cysteine is the least abundant amino acid in proteins; however, its importance is underlined by its presence in almost all proteins<sup>[1]</sup> and by the unique chemistry of its thiol group in cellular functions.<sup>[2]</sup> The diverse functional roles of cysteine include ubiquitylation,<sup>[3]</sup> caspase-mediated apoptosis,<sup>[4]</sup> maintenance of cellular redox potential,<sup>[5]</sup> defense against oxidative stress,<sup>[6]</sup> and contribution to redox signaling pathways,<sup>[7]</sup> as well as protein trafficking and localization.<sup>[8]</sup> The chemistry of the cysteine side chain is accountable for this broad range of functional roles.<sup>[9]</sup> The intrinsic properties of the thiol group, such as the large atomic radius of sulfur, environmental sensitivity of the  $pK_a$ , variable oxidation states,<sup>[6a,10]</sup> and metal chelating properties offer significant opportunities to accomplish the diverse functions of proteins.<sup>[1]</sup> Cysteine is also involved in various post-translational modifications, including alkylation, nitrosylation, and oxidation.<sup>[10]</sup> Furthermore, the thiol group can be oxidized to afford a disulfide bond in a dynamic and reversible fashion.<sup>[5]</sup> The cysteine–glutathione disulfide coupled system, a thiol-based redox switch, is a key component for the regulation of certain genes.<sup>[2c]</sup> In addition, the formation of a disulfide bond between two cysteine residues results in intra- or intermolecular linkages that can induce substantial changes in protein folding, thereby altering protein function.<sup>[11]</sup>

Homocysteine (Hcy) is an important intermediate in human metabolism and is being investigated as a biomarker for various cardiovascular diseases<sup>[12]</sup> and as a potential risk factor of Alzheimer's disease.<sup>[13]</sup> In contrast to cysteine, it is not translationally incorporated into proteins, but can be introduced through *N*-homocysteinylation<sup>[14]</sup> and *S*-homocysteinylation,<sup>[15]</sup> which have been proposed as factors for certain diseases.<sup>[16]</sup> Incorporation of homocysteine through *N*-homocysteinylation, for example, results in protein misfolding<sup>[17]</sup> and autoimmune response.<sup>[18]</sup> Further study of the relationship between homocysteine incorporation and protein function is thus needed to elucidate the mechanism of hyperhomocysteinemia and related diseases.<sup>[16]</sup>

Optical control of protein function provides spatial and temporal control over the activation and deactivation of cellular events, thereby enabling precise investigations of biological processes that cannot be accomplished with other conditional control elements.<sup>[19]</sup> We, and others, have previously developed an optochemical tool set for controlling protein function in live mammalian cells through the genetic encoding of photocaged versions of tyrosine and lysine.<sup>[20]</sup> We have applied those tools to the precise control of DNA recombination, protein localization, protein phosphorylation, kinase function nuclease activity, and DNA and RNA polymerase function.<sup>[21]</sup> Cys and Ser have previously been incorporated as direct nitrobenzyl thioethers and nitrobenzyl ethers, respectively, through tRNA synthetase engineering.<sup>[22]</sup> Here we are taking a different approach by engineering the molecular structure of caged cysteine and caged homocysteine for incorporation into proteins in bacterial and mammalian cells with the aid of an existing *M. barkeri* pyrrolysine tRNA synthetase (PylRS) mutant.<sup>[23]</sup>

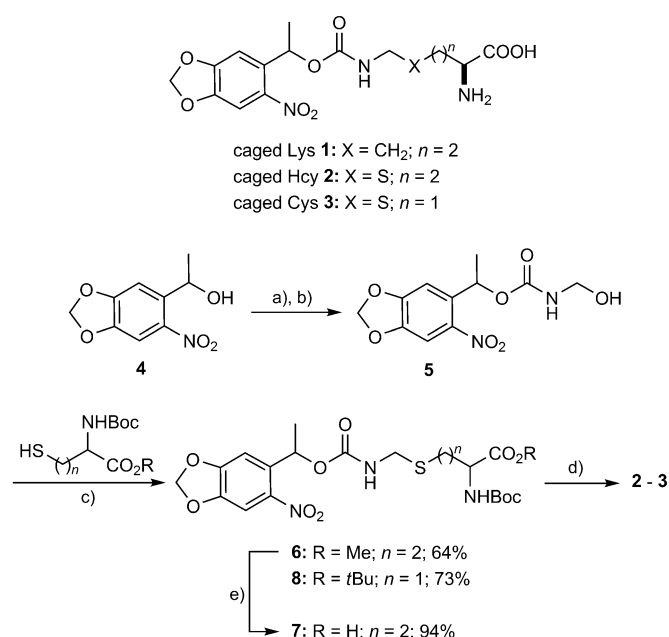
[a] Dr. R. Uprety, Prof. A. Deiters  
Department of Chemistry, North Carolina State University  
2620 Yarbrough Drive, Raleigh, NC 27695 (USA)

[b] J. Luo, J. Liu, Y. Naro, Dr. S. Samanta, Prof. A. Deiters  
Department of Chemistry, University of Pittsburgh  
219 Parkman Avenue, Pittsburgh, PA, 15260 (USA)  
E-mail: deiters@pitt.edu

 Supporting information for this article is available on the WWW under <http://dx.doi.org/10.1002/cbic.201400073>.

## Results and Discussion

Because the side chains of Cys and Hcy are significantly shorter than those of Lys and Tyr, we suspected that important contacts for amino acid recognition in the PylRS active site would be lost if traditional caging approaches were to be employed. We thus developed a “relay” caging/decaging strategy by inserting an additional aminomethylene spacer between the caging group and the thiol group of the amino acid. Photolysis of the *ortho*-nitrobenzyl group yields a carbamic acid. This carbamic acid rapidly decarboxylates, generating an unstable aminomethylene group that decarbonylates to release the active Cys or Hcy thiol. In this strategy, the caged Hcy **2** (Scheme 1)



**Scheme 1.** Structures of genetically encoded caged amino acids **1–3**. Synthetic routes to the “relay” caged homocysteine **2** and caged cysteine **3**. a) diphosgene, K<sub>2</sub>CO<sub>3</sub>, THF, then NH<sub>4</sub>OH; 83%; b) HCHO, K<sub>2</sub>CO<sub>3</sub>, DMSO; 70%; c) TsOH, dioxane; 70%; d) TES, TFA, DCM, RT, 77–78%; e) LiOH, dioxane.

displays a structure similar to that of the previously genetically encoded caged Lys **1**, with the exception of a subtle CH<sub>2</sub>→S modification. The caged Cys **3** has a very similar structure, shortened by just one methylene unit. We hypothesized that **2** and **3** should be substrates for the PylRS enzyme evolved for **1**.

The synthesis of caged homocysteine **2** was completed in five steps starting from the alcohol **4**, which was assembled by a literature procedure (Scheme 1).<sup>[24]</sup> The alcohol **4** was treated with diphosgene and subsequently with an excess of concentrated aqueous ammonia solution to form a carbamate in 83% yield.<sup>[25]</sup> The newly formed carbamate was subsequently treated with paraformaldehyde in the presence of 10 mol% K<sub>2</sub>CO<sub>3</sub> in DMSO to provide the hydroxymethyl carbamate **5** in 70% yield. The alcohol **5** underwent iminium ion chemistry through treatment with TsOH (8 mol%), and the iminium intermediate, generated in situ, was trapped by the thiol group of protected homocysteine<sup>[26]</sup> to deliver the product **6** in 64% yield. The

methyl ester was hydrolyzed with aqueous LiOH to give the corresponding acid **7** in 94% yield. Finally, Boc removal with TFA in CH<sub>2</sub>Cl<sub>2</sub> in the presence of triethylsilane (TES) furnished the caged homocysteine **2** in 78% yield.

The synthesis of the caged Cys followed the same approach; however, by switching from a methyl to a *tert*-butyl ester, the synthesis was shortened by one step and the iminium coupling yield for **5** to **8** was improved. Other amino acid protecting groups were explored as well, but only delivered diminished yields (data not shown).

In view of the designed structural similarity between **1–3**, the previously engineered synthetase for **1** (CKRS) was tested for the incorporation of **2** and **3**. CKRS has four mutations (M241F, A267S, Y271C, L274M) relative to the wild-type *MbPylRS* enzyme. In order to examine how these mutations might permit the incorporation of **2** and **3**, we first studied their effects on the interaction between the synthetase protein and the amino acid **1** by an in silico modeling approach. Utilizing MODELLER,<sup>[27]</sup> we generated the mutated protein, and then energy-minimized the structure with AMBER molecular dynamics.<sup>[28]</sup> Finally, we docked **1** into the active site binding pocket with AutoDock Vina.<sup>[29]</sup> The docked pose revealed that the Y271C and L274M mutations enlarge the pocket to accommodate the bulky bicyclic caging group, whereas M241F assists in orienting the aromatic nitrobenzyl ring in a favorable  $\pi$ -stacking interaction with W382 (Figure S3 in the Supporting Information). The A267S mutation provides an additional hydrogen bond through a water molecule to the amino acid carbonyl group, which, along with R295, assists in positioning the carboxylate group within the catalytically active site of CKRS.

In order to analyze the incorporation efficiencies of **1–3**, the plasmids pBAD-sfGFPY151TAG-pylT, containing a His<sub>6</sub>-tagged sfGFP gene with an amber stop codon at the Y151 permissive site, and pBK-CKRS, containing the gene encoding CKRS, were co-transformed into *Escherichia coli* Top10 cells. Cells were grown in lysogeny broth (LB) in the presence of the designated unnatural amino acid (1 mM), and protein expression was induced with arabinose (0.1%) when the OD<sub>600</sub> reached 0.4. Expression was continued at 37 °C overnight, followed by Ni-NTA purification. Importantly, all caged amino acids **1–3** could be incorporated into sfGFP at the Y151TAG mutation site (Figure 1A). Incorporation of **2** and **3** was further validated by ESI-MS of the purified caged-sfGFP (Figure S1), along with ESI-MS data for the decaged protein after light irradiation, confirming the expected fragmentation of the aminomethylene spacer (Figure S2).

According to the observed protein yields in *E. coli*, the incorporation efficiency of caged homocysteine **2** (1.5 mg L<sup>−1</sup>) is similar to that of caged lysine **1** (1.4 mg L<sup>−1</sup>), whereas the caged cysteine **3** gives a lower yield (0.9 mg L<sup>−1</sup>). To interpret the decreased incorporation efficiency for **3**, we compared the structures of **1–3** docked into the CKRS active site (Figure S4). The caged lysine **1** and caged homocysteine **2** adopted nearly identical conformations, yielding binding energies of −9.6 and −9.5 kJ mol<sup>−1</sup>, respectively. In previously reported native and mutant crystal structures of PylRS, it has been shown that N311 plays the role of a “gatekeeper”<sup>[30]</sup> and forms a crucial hy-

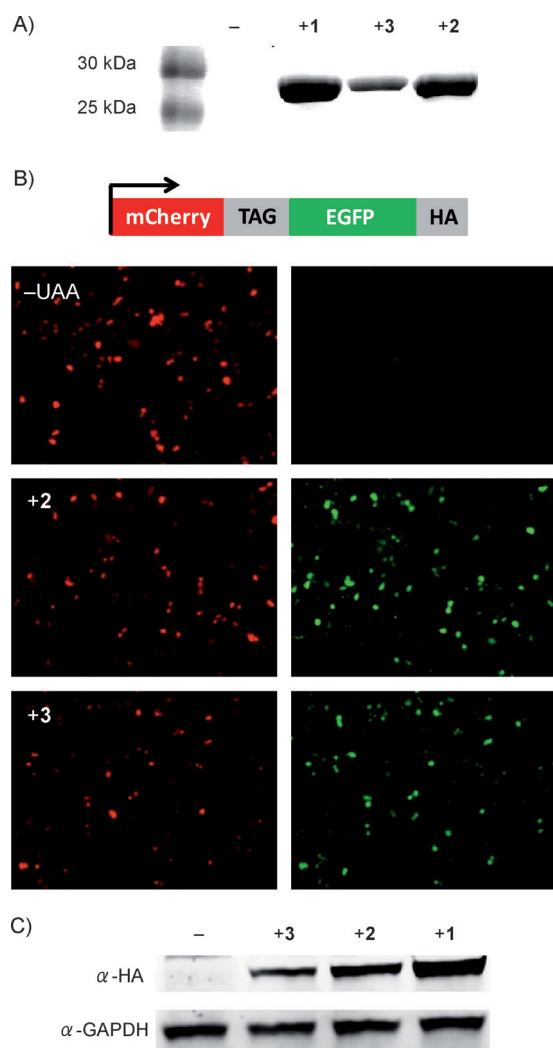


**Figure 1.** Genetic incorporation of photocaged lysine **1**, photocaged homocysteine **2**, and photocaged cysteine **3** in bacterial and mammalian cells. A) Coomassie-stained gel of Ni-NTA-purified sfGFP-Y151TAG expressed in *E. coli* in the absence and in the presence of **1**, **2**, and **3** (1 mM). B) Fluorescence micrographs of HEK293T cells expressing MbCKRS-mCherry-TAG-EGFP-HA and PyltRNA<sub>CUA</sub> in the absence and in the presence of **2** and **3** (1 mM). C) Western blot of lysate from HEK293T cells expressing mCherry-1/2/3-EGFP-HA with an anti-HA tag antibody and anti-GAPDH loading control confirms that the MbCKRS/PyItRNA<sub>CUA</sub> pair incorporates **1**, **2**, and **3** in response to the amber codon in mammalian cells.

drogen bond with the amide carbonyl group of pyrolysine.<sup>[23c,31]</sup> This interaction, together with a hydrogen bond between R295 and the carboxylate, plays a pivotal role in positioning the amino acid within the active site.<sup>[30a]</sup> The structures that resulted from our docking experiments for **1** and **2** shared these interactions, showing the formation of an H-bond between N311 and the carbamate carbonyl group, and another between the carboxylate group and R295. Docking of **3** produced two different conformations with slightly lower binding scores of  $-9.3$  and  $-9.2$  kJ mol<sup>-1</sup>. Because of the shorter length of the cysteine side chain, the caged cysteine **3** is unable to completely satisfy both interactions without compromise. Although the first conformation optimizes the interaction with N311, it does so at the cost of completely abolishing the

interaction with R295, placing the carboxylate group much further away from its ATP substrate. The second conformation does have this crucial interaction with R295, but at the cost of a weakened hydrogen bond with N311. The CKRS-bound **3** might exist in equilibrium between these two states, potentially leading to a decrease in catalytic activity and slightly reduced incorporation efficiency.

To demonstrate that the MbCKRS/PyItRNA<sub>CUA</sub> pair can direct the incorporation of **2** and **3** in response to an amber stop codon in mammalian cells, we co-transfected the plasmids pMbCKRS-mCherry-TAG-EGFP-HA and p4CMVE-U6-PyIT into human embryonic kidney (HEK) 293T cells in the presence and in the absence of **2** and **3**.<sup>[20b]</sup> As expected, mCherry fluorescence was observed in the cells either in the presence or in the absence of **2** and **3**, but EGFP fluorescence was detected only with the addition of **2** and **3** (Figure 1 B)—thus confirming the specificity of the synthetase. Western blot analysis further verified that the full-length mCherry-1/2/3-EGFP-HA fusion proteins were each expressed in the presence of **1**, **2**, or **3**. The relative ratio of expression of proteins incorporating **1**, **2**, and **3** is 3.0:1.5:1.0 (based on integration of the western blot bands with GE ImageQuant). These experiments demonstrate the successful incorporation of **2** and **3** into protein in response to the amber codon in mammalian cells (Figure 1 C).

In order to apply the caged amino acids **2** and **3** to trigger light-induced protein function in live mammalian cells, *Renilla* luciferase was selected as an initial target protein because its activity can be readily measured in cell culture and animal models.<sup>[32]</sup> By a different approach, firefly luciferase has previously been rendered light-activatable for temporal control of intracellular detection of ATP.<sup>[33]</sup> *Renilla* luciferase catalyzes the oxidation of coelenterazine in the presence of oxygen to generate coelenteramide and CO<sub>2</sub> with the concomitant emission of blue light (480 nm). The crystal structure of *Renilla* luciferase reveals that the conserved catalytic triad of D120, E144, and H285 is directly involved in the oxidation of coelenterazine (Figure 2 A). The cysteine C124 is located in close proximity to the “nucleophilic elbow” (residues 118–122) that is responsible for the positioning of D120 into the catalytic triad.<sup>[34]</sup> We hypothesized that introduction of the caged **3** at position C124 imposes steric hindrance on D120, and thus interferes with the formation of the catalytic triad blocking luciferase activity. A TAG mutation was introduced at position C124, and the incorporation of **2** and **3** was evaluated by co-transfecting HEK293T cells with the mutated *Renilla* luciferase plasmid (pRLuc-C124TAG) and plasmids encoding the MbCKRS/PyItRNA<sub>CUA</sub> pair. After a 24-hour incubation in the presence (1 mM) or in the absence of **2** and **3**, the cells were either irradiated for 4 min (365 nm, 25 W) or kept in the dark, followed by a *Renilla* luciferase assay. Confirming our hypothesis that incorporation of **2** and **3** in RLuc causes complete enzyme inactivity before UV irradiation, similar to the negative control in the absence of any unnatural amino acid. This demonstrates that the caging group was capable of fully inhibiting the function of the catalytic triad. After UV exposure, RLuc-**2** and -**3** were decaged, generating Hcy and Cys in the active site and restoring *Renilla* luciferase activity. A profound luminescence increase of 150-

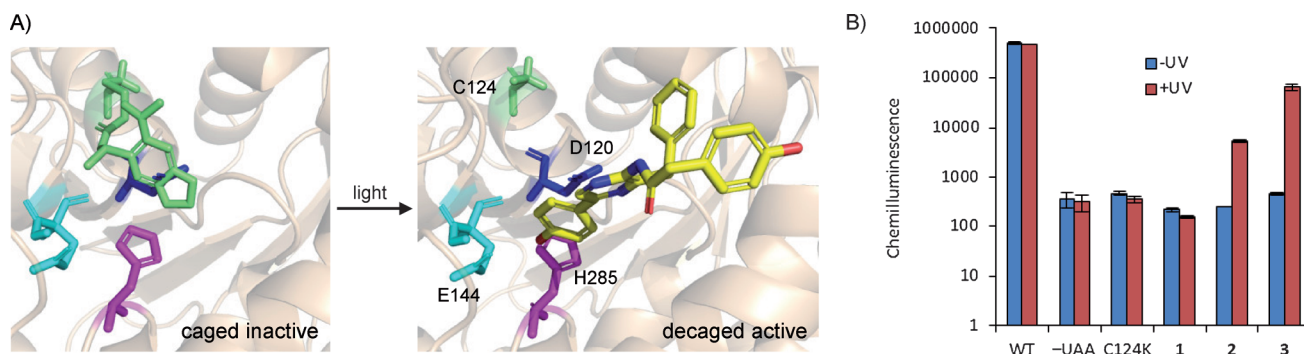


**Figure 2.** A) Structural analysis of optochemical control of *Renilla* luciferase. The photocaged cysteine **3** at the C124 position (green) and the catalytic triad of D120, E144, and H285 are shown (PDB ID: 2PSJ). Light-induced decaging allows access of the coelenterazine substrate (yellow) to the active site. B) In vivo light activation of *Renilla* luciferase containing **1**, **2**, and **3** at position C124. Chemiluminescence is shown on a logarithmic scale, indicating no activity of the caged enzyme and a > 150-fold activation after UV exposure of RLuc C124→**3**. Error bars represent standard deviations from three independent experiments.

fold was observed for **3**, because a wild-type active site containing Cys is obtained after photolysis of the caging group (Figure 2B). Only a 20-fold activity increase was seen on decaging of RLuc-2, despite the higher incorporation efficiency of **2** in mammalian cells (Figure 1C), because Hcy still perturbs the catalytic triad due to its CH<sub>2</sub>-extended side chain relative to Cys. Accordingly, the incorporation of the caged Lys **1** did not allow for light activation of luciferase activity, because the resulting C124K mutant is also completely inactive. These results confirm that decaging of **2** and **3** is functional in vivo, that protein activity can be controlled with caged cysteine and light in live cells, and that the incorporation of homocysteine allows for precise probing (with single-atom resolution) of protein active sites.

## Conclusions

In summary, the genetic code of bacterial and mammalian cells has been expanded by the genetic incorporation of photocaged homocysteine **2** and photocaged cysteine **3**. The design of the unnatural amino acids allowed for site-specific incorporation with the aid of an *MbPylCKRS* synthetase that had been developed by directed evolution to incorporate the structurally similar caged lysine **1**. The putative binding of the unnatural amino acids **1**–**3** to the mutant CKRS synthetase enzyme was investigated by in silico modeling; this revealed conformational differences that correspond well with incorporation efficiencies in vivo. Cysteine plays both structural and functional roles in many proteins and enzymes, and photochemical control over its activity should offer precise spatial and temporal regulation of a wide range of cellular processes. As a proof-of-principle, photochemical control of *Renilla* luciferase was achieved by caging the critical residue C124 through incorporation of **2** and **3** in live mammalian cells. Optochemical activation led to a 150-fold increase in enzymatic activity after brief UV illumination, thus demonstrating excellent OFF→ON switching behavior. Pyrrolysine-based genetic code expansion has also been successfully employed not only in bacterial and mammalian cells, but also in multicellular organisms.<sup>[35]</sup> Therefore, the genetically encoded caged cysteine analogues **2** and **3** should have broad and diverse optogenetic applications in various

biological systems. Beyond optochemical control, the site-specific incorporation of homocysteine into proteins should allow for precise investigation of the geometric requirements for transition states of cysteine-containing active sites.<sup>[36]</sup>

## Experimental Section

**Protein expression in *E. coli*:** sfGFP was amplified by PCR from pTrc-sfGFP-Y151TAG (gift from Dr. Ashton Cropp, Virginia Commonwealth University), digested with NcoI and NdeI (NEB), and ligated into the pBAD-Myo-4TAG-pyIT plasmid<sup>[23b]</sup> digested with the same restriction enzymes. The resulting plasmid, pBAD-sfGFP-Y151TAG-pyIT, was co-transformed with pBK-CKRS<sup>[20b]</sup> into *E. coli* Top10 cells. A single colony was grown in LB overnight, and the overnight culture (250 µL) was added to LB (25 mL) supplemented with the designated unnatural amino acid (1 mM), Tet (25 µg mL<sup>-1</sup>), and Kan (50 µg mL<sup>-1</sup>). Cells were grown at 37 °C, 250 rpm, and the protein expression was induced with arabinose (0.1%) when OD<sub>600</sub> reached 0.4. After overnight expression at 37 °C, cells were harvested and resuspended in phosphate lysis buffer (pH 8.0, 50 mM, 6 mL). Triton X-100 (60 µL, 10%) was added to the mixture. The lysate was incubated on ice for 1 h, sonicated, and then centrifuged (13 000 g) at 4 °C for 10 min. The supernatant was transferred to a 15 mL conical tube, and Ni-NTA resin (Qiagen, 100 µL) was added. The mixture was incubated at 4 °C for 2 h with mild shaking. The resin was then collected by centrifugation (1000 g, 10 min) and washed twice with lysis buffer (300 µL), followed by two washes with wash buffer (300 µL) containing imidazole (20 mM). The protein was eluted with elution buffer (300 µL) containing imidazole (250 mM). The purified proteins were analyzed by SDS-PAGE (10%), and stained with Coomassie Brilliant Blue. The protein mass was determined by electrospray ionization mass spectrometry (expected for caged homocysteine **2**: 28 482.4 Da; found: 28 481.8 Da; expected for caged cysteine **3**: 28 468.2 Da; found: 28 467.7 Da).

**Cell culture, plasmid transfection, and western blot:** Human embryonic kidney (HEK) 293T cells were grown in Dulbecco's Modified Eagle's Medium (DMEM, Gibco) supplemented with FBS (Gibco, 10%), Pen-Strep (Corning Cellgro, 1%) and L-glutamine (Alfa Aesar, 2 mM) in 96-well plates (Costar) under a humidified atmosphere containing CO<sub>2</sub> (5%) at 37 °C. HEK293T cells were transiently transfected with pMbCKRS-mCherry-TAG-EGFP-HA and p4CMVE-U6-PyIT<sup>[20b]</sup> (gifts from the Chin lab, Medical Research Council Laboratory of Molecular Biology) at ≈75% confluency in the presence or in the absence of **2** and **3** (1 mM) in 96-well plates. Double trans-



fections were performed with equal amounts of two plasmids. After incubation (37 °C) overnight, the cells were washed with PBS and imaged with a Zeiss Axio Observer.Z1 Microscope (10× objective). To confirm the expression of the fusion protein, and also to differentiate between expression levels, a western blot was performed. HEK293T cells were co-transfected with pMbCKRS-mCherry-TAG-EGFP-HA and p4CMVE-U6-PyIT in the presence or in the absence of **2** and **3** (1 mM) in 6-well plates. After 24 h of incubation, the cells were washed with chilled PBS and lysed in mammalian protein extraction buffer (GE Healthcare) with complete protease inhibitor cocktail (Sigma) on the ice shaker, and the cell lysates were then quantified, isolated, and extracted at 12000g centrifugation (4 °C, 20 min). The protein lysate was boiled with SDS and then analyzed by SDS-PAGE (10%). After gel electrophoresis and transfer to nitrocellulose membrane (GE Healthcare), the membrane was blocked in TBS with Tween 20 (Fisher Scientific, 0.1%) and milk powder (5%) for 1 h. The blots were probed and incubated with the primary antibody [ $\alpha$ -HA-probe (Y-11) rabbit polyclonal IgG (sc-805, Santa Cruz Biotech)] overnight at 4 °C, followed with the fluorescent secondary antibody [goat- $\alpha$ -rabbit IgG Cy3 (GE Healthcare)] for 1 h at room temperature. The binding and washing steps were performed in TBS with Tween 20 (0.1%).

**Photocaged *Renilla* luciferase assay:** HEK293T cells were cultured in DMEM (Gibco) supplemented with FBS (Gibco, 10%), Pen-Strep (Gibco, 1%) and L-glutamine (Alfa Aesar, 2 mM) in 96-well plates (BD Falcon) under a humidified atmosphere containing CO<sub>2</sub> (5%) at 37 °C. At 80–90% confluency, cells seeded on plates were transfected, and medium was changed to fresh DMEM or DMEM supplemented with **1**, **2**, or **3** (1 mM). The plasmid pAG31–38, containing both pCMV-MbCKRS and p4CMVE-U6-PyIT, was constructed. A TAG amber stop codon was introduced into the C124 site by use of the QuikChange mutagenesis kit (Agilent Technologies) and primers For (gccacgactgggggcttagctggtcttctactctc) and Rev (gagtagtgaaaggccagctaagccccccagctgctggc). A pRL-TK plasmid containing the gene encoding *Renilla* luciferase with a TAG amber mutation at residue C124 (pRL-C124TAG) was co-transfected into cells with the plasmid pAG31–38 by use of BPEI according to the manufacturer's protocols (Sigma). After double transfection and incubation (24 h), the medium was changed to DMEM without phenol red, and cells were then irradiated with UV light (365 nm) for 4 min with a 365 nm UV lamp (high-performance UV transilluminator, UVP, 25 W). HEK293T cells expressing RLuc-C124TAG or RLuc-1/2/3 were lysed with lysis buffer (Promega, 20  $\mu$ L) with and without UV irradiation on the shaker. Cell lysates (20  $\mu$ L) were mixed with coelenterazine substrate solution (Promega, 100  $\mu$ L) in a 96-well plate (BD Falcon). The luciferase activity was measured by use of the *Renilla* luciferase assay system (Promega) and a Synergy 4 Multi-mode Microplate Reader with integration time 2 s and sensitivity at 150.

**Mutant structure generation and energy minimization:** The initial structure of PDB ID 2Q7H was chosen as a starting point for the modeling. The missing loops were remodeled with MODELLER, followed by insertion of the four point mutations M241F, A267S, Y271C, and L274M with the *mutate\_model.py* script provided by the MODELLER software. Superposition of PDB ID 2Q7G onto 2Q7H provided the coordinates for the incorporation of ATP and magnesium ions into the mutant structure. The ATP and magnesium ions were parameterized in *antechamber* by use of previously developed parameters.<sup>[37]</sup> This mutant complex was then imported into AMBER 12 molecular dynamics software with use of the AMBER FF99SBILDN force field.<sup>[38]</sup> The protein was placed into a cubic box with a 12.0 Å border, solvated with 14695 water molecules, and charge-neutralized with the addition of six sodium ions. This

system was energy-minimized with 5000 steps of steepest descent, and 5000 steps of a conjugate gradient method with 8 kcal mol<sup>−1</sup> area<sup>2</sup> restraints placed on all residues and ligands except for the newly generated point mutations. This was followed by an additional 5000 steps steepest descent and 15000 steps conjugate gradient with a 3 kcal mol<sup>−1</sup> area<sup>2</sup> restraint placed on all residues and ligands to produce the starting structure for our docking experiments. All computational experiments were completed on the Center for Simulation and Modeling (SAM) Frank supercomputer at the University of Pittsburgh.

**Molecular docking experiments:** The energy-minimized mutant structure was prepared for docking with *AutoDock Vina* by removing all sodium ions and all water molecules except for a single water molecule situated in the active-site pocket of the protein. This structural water molecule is present in all available crystal structures and plays an important role in amino acid recognition. The receptor input file was prepared with the *prepare\_receptor4.py* script provided by the *AutoDock Tools* software.<sup>[39]</sup> The unnatural amino acid ligands were constructed with ChemBioDraw3D, and the molecular geometry was optimized with the MMFF94 force field.<sup>[40]</sup> The ligand input files were prepared for docking with the *prepare\_ligand4.py* script of *AutoDock Tools*. All docking experiments were run with exhaustiveness set to 8. Initial docking results were then subjected to an additional round of energy minimization of the pYLRS-UAA complex with AMBER 12. The complex was minimized with 5000 steps steepest descent, 15000 steps conjugate gradient with 8 kcal mol<sup>−1</sup> area<sup>2</sup> restraints placed on the protein, with the UAA left unrestrained. This was followed by an additional 5000 steps steepest descent, and 15000 steps conjugate gradients with no restraints on protein or ligands. This relaxed pYLRS-UAA complex structure was then re-docked to produce the final docked structures.

**1-(6-Nitrobenzo[d][1,3]dioxol-5-yl)ethyl (hydroxymethyl)carbamate (5):** Diphosgene (1.20 mL, 10.4 mmol) and K<sub>2</sub>CO<sub>3</sub> (2.50 g, 18.8 mmol) were added to a solution of the alcohol **4** (2.0 g, 9.4 mmol) in dry THF (30 mL), with stirring at 0 °C under an inert atmosphere. Stirring was continued for 12 h, and the reaction mixture was allowed to warm to room temperature. The reaction mixture was concentrated under reduced pressure, CH<sub>2</sub>Cl<sub>2</sub> (50 mL) was added, and the organic layer was washed with brine (2×20 mL). The organic layer was dried over anhydrous Na<sub>2</sub>SO<sub>4</sub> and filtered. The filtrate was concentrated under reduced pressure, and the residue was dissolved in THF (20 mL). The solution was cooled to 0 °C in an ice bath, followed by addition of a concentrated aqueous solution of ammonium hydroxide (20 mL, 14.8 M) with vigorous stirring to precipitate the crude product. Stirring was continued for 2 h at the same temperature to induce complete precipitation. The volatiles were then removed under reduced pressure to minimize loss of product (because of its partial solubility in THF), and the precipitate was collected by filtration. The precipitate was washed with water (5×30 mL) and dried under high vacuum to furnish the carbamate intermediate (1.7 g, yield 89%) as a yellow solid. M.p. 189–190 °C; <sup>1</sup>H NMR (400 MHz, [D<sub>6</sub>]DMSO):  $\delta$  = 7.57 (s, 1H), 7.08 (s, 1H), 6.75 (br, 1H), 6.51 (br, 1H), 6.23–5.91 (m, 1H), 1.46 ppm (d, *J* = 3.4 Hz, 3H); <sup>13</sup>C NMR (100 MHz, [D<sub>6</sub>]DMSO):  $\delta$  = 155.6, 152.2, 146.9, 141.1, 135.8, 105.4, 104.6, 103.5, 66.7, 21.7 ppm.

Paraformaldehyde (130 mg, 4.32 mmol) and K<sub>2</sub>CO<sub>3</sub> (67 mg, 0.48 mmol) were added to a solution of the carbamate intermediate (1.00 g, 3.93 mmol) in dry DMSO (10 mL), with stirring at room temperature under an inert atmosphere. Stirring was continued for 2 h. EtOAc (40 mL) and brine (40 mL) were added to the reaction mixture. The organic layer was separated, and the aqueous layer

was extracted with EtOAc (2×20 mL). The organic layers were combined, washed with brine (2×20 mL), dried over anhydrous Na<sub>2</sub>SO<sub>4</sub>, and filtered. The filtrate was concentrated, and the remaining crude product was purified by column chromatography on silica gel with acetone/CH<sub>2</sub>Cl<sub>2</sub> (1:7) to furnish **5** (780 mg, yield 70%) as a white solid. <sup>1</sup>H NMR (300 MHz, [D<sub>6</sub>]DMSO): δ = 7.98 (t, *J* = 6.3 Hz, 1H), 7.57 (s, 1H), 7.09 (s, 1H), 6.22 (s, 2H), 6.02–5.54 (m, 1H), 5.57 (t, *J* = 6.6 Hz, 1H), 4.35 (t, *J* = 6.6 Hz, 1H), 1.50 ppm (s, *J* = 3.1 Hz, 3H); <sup>13</sup>C NMR (75 MHz, [D<sub>6</sub>]DMSO): δ = 155.0, 152.2, 147.0, 141.2, 135.4, 105.5, 104.6, 103.5, 67.1, 64.3, 21.7 ppm; LRMS (ESI): *m/z* calcd for C<sub>11</sub>H<sub>12</sub>N<sub>2</sub>O<sub>7</sub>Na: 307.05 [*M*+Na]<sup>+</sup>; found: 307.00.

**Methyl 2-[(*tert*-butoxycarbonyl)amino]-4-[[[1-(6-nitrobenzo[d]-[1,3]dioxol-5-yl)ethoxy]carbonyl]amino)methyl]thio]butanoate**

**(6):** *N*-Boc-homocysteine methyl ester (270 mg, 1.03 mmol) and TsOH (16 mg, 0.08 mmol) were added to a solution of alcohol **5** (1.00 g, 3.93 mmol) in dry dioxane (5 mL), with stirring at room temperature under an inert atmosphere. Stirring was continued for another 14 h, EtOAc (20 mL) was added to the reaction mixture, and the organic layer was washed with a saturated aqueous solution of NaHCO<sub>3</sub> (2×20 mL) and brine (2×20 mL), dried over anhydrous Na<sub>2</sub>SO<sub>4</sub>, and filtered. The filtrate was concentrated under reduced pressure, and the crude product was purified by column chromatography on silica gel with Et<sub>2</sub>O/CH<sub>2</sub>Cl<sub>2</sub> (1:4) to yield **6** (316 mg, yield 64%) as an oil. <sup>1</sup>H NMR (300 MHz, CDCl<sub>3</sub>): δ = 7.48 (s, 1H), 6.99 (s, 1H), 6.31–6.25 (q, 1H), 6.11 (s, 2H), 5.46 (br, 1H), 5.19 (br, 1H), 4.38–4.16 (m, 4H), 3.75 (s, 3H), 2.73–2.54 (m, 2H), 2.07–1.88 (m, 2H), 1.58 (d, *J* = 3.3 Hz, 3H), 1.44 ppm (s, 9H); <sup>13</sup>C NMR (75 MHz, CDCl<sub>3</sub>): δ = 172.9, 155.2, 152.6, 147.3, 141.6, 136.3, 105.5, 105.3, 105.2, 80.4, 69.6, 65.9, 52.7, 43.3, 34.6, 32.7, 28.5, 27.1, 22.3 ppm; LRMS (ESI): *m/z* calcd for C<sub>21</sub>H<sub>29</sub>N<sub>3</sub>O<sub>10</sub>Na: 538.14 [*M*+Na]<sup>+</sup>; found: 538.10.

**2-[(*tert*-Butoxycarbonyl)amino]-4-[[[1-(6-nitrobenzo[d][1,3]dioxol-5-yl)ethoxy]carbonyl]amino)methyl]thio]butanoic acid** (**7**): An aqueous solution of LiOH (2 mL, 2 M) was added to a solution of methyl ester **6** (300 mg, 0.580 mol) in dry dioxane (2 mL), with stirring at 0 °C under an inert atmosphere. Stirring was continued for 30 min. Water (20 mL) was added to the reaction mixture, the aqueous layer was washed with Et<sub>2</sub>O (10 mL), and the organic layer was discarded. Next, the aqueous layer was acidified to pH 3.0 with an aqueous solution of citric acid (5%). The product remaining in the aqueous layer was then extracted with EtOAc (2×20 mL). The combined organic layers were washed with brine (2×20 mL), dried over anhydrous Na<sub>2</sub>SO<sub>4</sub>, and filtered. The filtrate was concentrated to dryness under reduced pressure to afford **7** (275 mg, yield 94%) as a yellow foam. <sup>1</sup>H NMR (400 MHz, CDCl<sub>3</sub>): δ = 7.48 (s, 1H), 7.00 (s, 1H), 6.27–6.26 (m, 1H), 6.10 (s, 2H), 5.57 (s, 1H), 5.46–5.36 (m, 1H), 4.36–4.21 (m, 3H), 2.78–2.65 (br, 2H), 2.11–1.96 (br, 2H), 1.57 (d, *J* = 3.2 Hz, 3H), 1.4 ppm (s, 9H); <sup>13</sup>C NMR (100 MHz, CDCl<sub>3</sub>): δ = 176.0, 152.6, 147.3, 141.6, 136.2, 105.8, 105.4, 103.3, 70.7, 69.7, 65.9, 52.6, 43.4, 32.5, 28.5, 27.3, 22.3 ppm; LRMS (ESI): *m/z* calcd for C<sub>20</sub>H<sub>27</sub>N<sub>3</sub>O<sub>10</sub>Na: 524.13 [*M*+Na]<sup>+</sup>; found: 524.10.

**2-Amino-4-[[[1-(6-nitrobenzo[d][1,3]dioxol-5-yl)ethoxy]carbonyl]amino)methyl]thio]butanoic acid** (**2**): Triethylsilane (644 μL, 2.34 mmol) and caged Boc-homocysteine **7** (1.0 g, 1.9 mmol) were added to TFA/CH<sub>2</sub>Cl<sub>2</sub> (1:1, 18 mL), and the mixture was stirred at room temperature for 45 min under an inert atmosphere. It was then concentrated under reduced pressure, and the residue was dissolved in MeOH (10 mL). To remove the residual amount of TFA completely from the reaction mixture, the mixture was again concentrated under reduced pressure, and the residue was redissolved in MeOH. The process was subsequently repeated three times. Fi-

nally, the solid was dissolved in MeOH (2 mL) and added dropwise to Et<sub>2</sub>O (200 mL) with vigorous stirring to precipitate the crude product. The process of dissolving the product followed by precipitation was repeated twice to afford the caged homocysteine TFA salt **2** (800 mg, yield 78%) as a crystalline white solid. <sup>1</sup>H NMR (400 MHz, CD<sub>3</sub>OD): δ = 7.48 (d, *J* = 2.8 Hz, 1H), 7.11–7.09 (m, 1H), 6.20–6.13 (m, 3H), 4.25–4.14 (m, 2H), 3.86–3.77 (m, 2H), 2.87 (br, 1H), 2.69–1.67 (br, 2H), 2.22 (br, 1H), 2.07 (br, 1H), 1.63–1.59 ppm (m, 3H); <sup>13</sup>C NMR (100 MHz, CD<sub>3</sub>OD): δ = 172.9, 157.7, 154.1, 148.9, 143.0, 137.1, 106.6, 105.9, 105.0, 70.3, 53.9, 43.4, 32.1, 27.2, 22.4 ppm; LRMS (ESI): *m/z* calcd for C<sub>15</sub>H<sub>20</sub>N<sub>3</sub>O<sub>8</sub>S: 402.09 [*M*+Na]<sup>+</sup>; found: 402.09.

**(2*R*)-*tert*-Butyl 2-[(*tert*-butoxycarbonyl)amino]-3-[[[1-(6-nitrobenzo[d][1,3]dioxol-5-yl)ethoxy]carbonyl]amino)methyl]thio]propanoate** (**8**): *N*-Boc-cysteine *tert*-butyl ester (421 mg, 1.52 mmol) and TsOH (24 mg, 0.12 mmol) were added to a solution of the alcohol **5** (360 mg, 1.26 mmol) in dry dioxane (5 mL), with stirring at room temperature under an inert atmosphere. Stirring was continued for 12 h. The reaction mixture was diluted with EtOAc (20 mL), and the organic layer was washed with a saturated aqueous solution of NaHCO<sub>3</sub> (2×20 mL) and brine (20 mL), dried over anhydrous Na<sub>2</sub>SO<sub>4</sub>, and filtered. The filtrate was concentrated under reduced pressure, and the obtained crude product was purified by column chromatography on silica gel with Et<sub>2</sub>O/CH<sub>2</sub>Cl<sub>2</sub> (1:9) to deliver **8** (505 mg, yield 73%) as an oil. <sup>1</sup>H NMR (300 MHz, CDCl<sub>3</sub>): δ = 7.47 (s, 1H), 7.02 (s, 1H), 6.28 (br, 1H), 6.09 (s, 2H), 5.79 (br, 1H), 5.35 (br, 1H), 4.36–4.17 (m, 3H), 3.04–3.00 (m, 1H), 2.92–2.89 (m, 1H), 1.58 (br, 3H), 1.56 ppm (s, 18H); <sup>13</sup>C NMR (75 MHz, CDCl<sub>3</sub>): δ = 170.1, 154.9, 152.6, 147.2, 141.5, 136.4, 105.8, 105.4, 103.2, 83.1, 80.5, 69.5, 54.4, 44.6, 34.7, 28.5, 28.1, 22.4 ppm; LRMS (ESI): *m/z* calcd for C<sub>23</sub>H<sub>33</sub>N<sub>3</sub>O<sub>10</sub>Na: 566.1788 [*M*+Na]<sup>+</sup>; found: 566.1784.

**(2*R*)-2-Amino-3-[[[1-(6-nitrobenzo[d][1,3]dioxol-5-yl)ethoxy]carbonyl]amino)methyl]thio]propanoic acid** (**3**): Triethylsilane (311 μL, 1.90 mmol) and the caged Boc-cysteine **7** (525 mg, 0.960 mmol) were added to a solution of TFA/CH<sub>2</sub>Cl<sub>2</sub> (1:1, 10 mL), with stirring at room temperature under an inert atmosphere. Stirring was continued for 45 min. The reaction mixture was concentrated under reduced pressure, the obtained residue was redissolved in MeOH (5 mL), and the process of dissolution and concentration was repeated twice to remove residual amounts of TFA. Finally, the crude product was dissolved in MeOH (1 mL), and the solution was added dropwise to Et<sub>2</sub>O (100 mL) with vigorous stirring to precipitate the crude product. The precipitate was redissolved in MeOH (1 mL), and the process of precipitation was repeated once more to afford the caged cysteine TFA salt **3** (370 mg, yield 77%) as a crystalline hygroscopic white solid. <sup>1</sup>H NMR (300 MHz, CD<sub>3</sub>OD): δ = 7.48 (s, 1H), 7.10 (s, 1H), 6.23–6.16 (m, 1H), 6.14 (s, 2H), 4.30–4.20 (m, 2H), 3.89–3.85 (m, 1H), 3.24–3.15 (m, 1H), 2.99–2.91 (m, 1H), 1.57 ppm (d, *J* = 3.1 Hz, 3H); <sup>13</sup>C NMR (75 MHz, CD<sub>3</sub>OD): δ = 172.4, 157.6, 154.2, 149.0, 143.1, 137.2, 106.7, 106.0, 105.1, 70.5, 54.9, 44.1, 32.7, 28.3, 22.5 ppm; LRMS (ESI): *m/z* calcd for C<sub>14</sub>H<sub>18</sub>N<sub>3</sub>O<sub>8</sub>S: 379.14 [*M*+H]<sup>+</sup>; found: 379.15.

## Acknowledgements

This work was support in part by the National Science Foundation (CHE-0848398) and the University of Pittsburgh.

**Keywords:** amino acids • caged compounds • cysteine • gene technology • homocysteine • protein modifications

- [1] N. J. Pace, E. Weerapana, *ACS Chem. Biol.* **2013**, *8*, 283–296.
- [2] a) Y. Kim, S. O. Ho, N. R. Gassman, Y. Korlann, E. V. Landorf, F. R. Collart, S. Weiss, *Bioconjugate Chem.* **2008**, *19*, 786–791; b) E. Baslé, N. Joubert, M. Pucheault, *Chem. Biol.* **2010**, *17*, 213–227; c) H. Antelmann, J. D. Hellmann, *Antioxid. Redox Signaling* **2011**, *14*, 1049–1063; d) K. G. Reddie, K. S. Carroll, *Curr. Opin. Chem. Biol.* **2008**, *12*, 746–754.
- [3] a) L. Spasser, A. Brik, *Angew. Chem. Int. Ed.* **2012**, *51*, 6840–6862; *Angew. Chem.* **2012**, *124*, 6946–6969; b) T. Tasaki, Y. T. Kwon, *Trends Biochem. Sci.* **2007**, *32*, 520–528.
- [4] a) M. Lamkanfi, N. Festjens, W. Declercq, T. Vanden Berghe, P. Vandenabeele, *Cell Death Differ.* **2007**, *14*, 44–55; b) S. J. Riedl, Y. Shi, *Nat. Rev. Mol. Cell Biol.* **2004**, *5*, 897–907.
- [5] M. Kemp, Y. M. Go, D. P. Jones, *Free Radical Biol. Med.* **2008**, *44*, 921–937.
- [6] a) L. E. Netto, M. A. de Oliveira, G. Monteiro, A. P. Demasi, J. R. Cussiol, K. F. Discola, M. Demasi, G. M. Silva, S. V. Alves, V. G. Faria, B. B. Horta, *Comp. Biochem. Physiol. C* **2007**, *146*, 180–193; b) L. E. Shao, T. Tanaka, R. Gribi, J. Yu, *Ann. N. Y. Acad. Sci.* **2002**, *962*, 140–150; c) D. P. Jones, *Am. J. Physiol. Cell Physiol.* **2008**, *295*, C849–868; d) R. S. Balaban, S. Nemoto, T. Finkel, *Cell* **2005**, *120*, 483–495; e) T. Finkel, *Nat. Rev. Mol. Cell Biol.* **2005**, *6*, 971–976.
- [7] a) A. Delaunay, D. Pflieger, M. B. Barrault, J. Vinh, M. B. Toledano, *Cell* **2002**, *111*, 471–481; b) Y. Collins, E. T. Chouchani, A. M. James, K. E. Menger, H. M. Cocheme, M. P. Murphy, *J. Cell Sci.* **2012**, *125*, 801–806.
- [8] a) G. Bastin, K. Singh, K. Dissanayake, A. S. Mighiu, A. Nurmohamed, S. P. Heximer, *J. Biol. Chem.* **2012**, *287*, 28966–28974; b) J. Greaves, L. H. Chamberlain, *J. Cell Biol.* **2007**, *176*, 249–254; c) J. E. Smotrys, M. E. Linder, *Annu. Rev. Biochem.* **2004**, *73*, 559–587; d) A. Higdon, A. R. Diers, J. Y. Oh, A. Landar, V. M. Darley-Usmar, *Biochem. J.* **2012**, *442*, 453–464.
- [9] M. Lindahl, A. Mata-Cabana, T. Kieselbach, *Antioxid. Redox Signaling* **2011**, *14*, 2581–2642.
- [10] N. M. Giles, G. I. Giles, C. Jacob, *Biochem. Biophys. Res. Commun.* **2003**, *300*, 1–4.
- [11] D. Fass, *Annu. Rev. Biophys. Bioeng.* **2012**, *41*, 63–79.
- [12] A. S. Wierzbicki, *Diab. Dis. Res.* **2007**, *4*, 143–150.
- [13] S. Seshadri, A. Beiser, J. Selhub, P. F. Jacques, I. H. Rosenberg, R. B. D'Agostino, P. W. F. Wilson, P. A. Wolf, *New Engl. J. Med.* **2002**, *346*, 476–483.
- [14] H. Jakubowski, *J. Biol. Chem.* **1997**, *272*, 1935–1942.
- [15] A. V. Glushchenko, D. W. Jacobsen, *Antioxid. Redox Signaling* **2007**, *9*, 1883–1898.
- [16] H. Jakubowski, *J. Nutr.* **2006**, *136*, 1741S–1749S.
- [17] P. Paoli, F. Sbrana, B. Tiribilli, A. Caselli, B. Pantera, P. Cirri, A. De Donatis, L. Formigli, D. Nosi, G. Manao, G. Camici, G. Ramponi, *J. Mol. Biol.* **2010**, *400*, 889–907.
- [18] A. Undas, J. Perla, M. Laciniski, W. Trzeciak, R. Kazmierski, H. Jakubowski, *Stroke* **2004**, *35*, 1299–1304.
- [19] a) H. M. Lee, D. R. Larson, D. S. Lawrence, *ACS Chem. Biol.* **2009**, *4*, 409–427; b) A. Deiters, *ChemBioChem* **2010**, *11*, 47–53; c) C. W. Riggsbee, A. Deiters, *Trends Biotechnol.* **2010**, *28*, 468–475; d) L. Gardner, A. Deiters, *Curr. Opin. Chem. Biol.* **2012**, *16*, 292–299; e) C. Brieke, F. Rohrbach, A. Gottschalk, G. Mayer, A. Heckel, *Angew. Chem. Int. Ed.* **2012**, *51*, 8446–8476; *Angew. Chem.* **2012**, *124*, 8572–8604.
- [20] a) A. Deiters, D. Groff, Y. Ryu, J. Xie, P. G. Schultz, *Angew. Chem. Int. Ed.* **2006**, *45*, 2728–2731; *Angew. Chem.* **2006**, *118*, 2794–2797; b) A. Gautier, D. P. Nguyen, H. Lusic, W. An, A. Deiters, J. W. Chin, *J. Am. Chem. Soc.* **2010**, *132*, 4086–4088; c) Y.-S. Wang, B. Wu, Z. Wang, Y. Huang, W. Wan, W. K. Russell, P.-J. Pai, Y. N. Moe, D. H. Russell, W. R. Liu, *Mol. Biosyst.* **2010**, *6*, 1557–1560; d) D. Groff, P. R. Chen, F. B. Peters, P. G. Schultz, *ChemBioChem* **2010**, *11*, 1066–1068.
- [21] a) W. F. Edwards, D. D. Young, A. Deiters, *ACS Chem. Biol.* **2009**, *4*, 441–445; b) C. Chou, D. D. Young, A. Deiters, *Angew. Chem. Int. Ed.* **2009**, *48*, 5950–5953; *Angew. Chem.* **2009**, *121*, 6064–6067; c) C. Chou, D. D. Young, A. Deiters, *ChemBioChem* **2010**, *11*, 972–977; d) C. Chou, A. Deiters, *Angew. Chem. Int. Ed.* **2011**, *50*, 6839–6842; *Angew. Chem.* **2011**, *123*, 6971–6974; e) A. Gautier, A. Deiters, J. W. Chin, *J. Am. Chem. Soc.* **2011**, *133*, 2124–2127; f) E. Arbely, J. Torres-Kolbus, A. Deiters, J. W. Chin, *J. Am. Chem. Soc.* **2012**, *134*, 11912–11915; g) J. Hemphill, C. Chou, J. W. Chin, A. Deiters, *J. Am. Chem. Soc.* **2013**, *135*, 13433–13439.
- [22] a) N. Wu, A. Deiters, T. A. Cropp, D. King, P. G. Schultz, *J. Am. Chem. Soc.* **2004**, *126*, 14306–14307; b) E. A. Lemke, D. Summerer, B. H. Geierstanger, S. M. Brittain, P. G. Schultz, *Nat. Chem. Biol.* **2007**, *3*, 769–772; c) J.-Y. Kang, D. Kawaguchi, I. Coin, Z. Xiang, D. D. M. O'Leary, P. A. Slesinger, L. Wang, *Neuron* **2013**, *80*, 358–370; d) D. P. Nguyen, M. Mahesh, S. J. Elsäasser, S. M. Hancock, C. Uttamapinant, J. W. Chin, *J. Am. Chem. Soc.* **2014**, *136*, 2240–2243.
- [23] a) W. Wan, J. M. Tharp, W. R. Liu, *Biochim. Biophys. Acta Proteins Proteomics* **2014**, *1844*, 1059–1070; b) H. Neumann, S. Y. Peak-Chew, J. W. Chin, *Nat. Chem. Biol.* **2008**, *4*, 232–234; c) T. Yanagisawa, R. Ishii, R. Fukunaga, T. Kobayashi, K. Sakamoto, S. Yokoyama, *Chem. Biol.* **2008**, *15*, 1187–1197; d) P. R. Chen, D. Groff, J. Guo, W. Ou, S. Cellitti, B. H. Geierstanger, P. G. Schultz, *Angew. Chem. Int. Ed.* **2009**, *48*, 4052–4055; *Angew. Chem.* **2009**, *121*, 4112–4115; e) D. P. Nguyen, H. Lusic, H. Neumann, P. B. Kapadnis, A. Deiters, J. W. Chin, *J. Am. Chem. Soc.* **2009**, *131*, 8720–8721; f) C. J. Chou, R. Uprety, L. Davis, J. W. Chin, A. Deiters, *Chem. Sci.* **2011**, *2*, 480–483; g) C. H. Kim, M. Kang, H. J. Kim, A. Chatterjee, P. G. Schultz, *Angew. Chem. Int. Ed.* **2012**, *51*, 7246–7249; *Angew. Chem.* **2012**, *124*, 7358–7361; h) K. Lang, L. Davis, J. Torres-Kolbus, C. Chou, A. Deiters, J. W. Chin, *Nat. Chem.* **2012**, *4*, 298–304.
- [24] E. Anderson, T. Brown, D. Picken, *Nucleosides Nucleotides Nucleic Acids* **2003**, *22*, 1403–1406.
- [25] C. Z. Ding, R. B. Silverman, *Synth. Commun.* **1993**, *23*, 1467–1471.
- [26] a) I. S. Weitz, M. Pellegrini, D. F. Mierke, M. Chorev, *J. Org. Chem.* **1997**, *62*, 2527–2534; b) C. E. McInnis, H. E. Blackwell, *Bioorg. Med. Chem.* **2011**, *19*, 4820–4828.
- [27] N. Eswar, B. Webb, M. A. Marti-Renom, M. S. Madhusudhan, D. Eramian, M. Y. Shen, U. Pieper, A. Sali, *Curr. Protoc. Bioinf.* **2006**, Unit 5 6.
- [28] T. A. Darden, D. A. Case, T. E. Cheatham III, C. L. Simmerling, J. Wang, R. E. Duke, R. Luo, R. C. Walker, W. Zhang, K. M. Merz, B. Roberts, S. Hayik, A. Roitberg, G. Seabra, J. Swails, A. W. Goetz, I. Kolossvary, K. F. Wong, F. Paesani, J. Vanicek, R. M. Wolf, J. Liu, X. Wu, S. R. Brozell, T. Steinbrecher, H. Gohlke, Q. Cai, X. Ye, J. Wang, M.-J. Hsieh, G. Cui, D. R. Roe, D. H. Mathews, M. G. Seetin, R. Salomon-Ferrer, C. Sagui, V. Babin, T. Luchko, S. Gusarov, A. Kovalenko, P. A. Kollman in *AMBER 12*, University of California, San Francisco, San Francisco, CA, **2012**.
- [29] O. Trott, A. J. Olson, *J. Comput. Chem.* **2010**, *31*, 455–461.
- [30] a) J. M. Kavran, S. Gundllapalli, P. O'Donoghue, M. Englert, D. Soll, T. A. Steitz, *Proc. Natl. Acad. Sci. USA* **2007**, *104*, 11268–11273; b) J. K. Takimoto, N. Dellas, J. P. Noel, L. Wang, *ACS Chem. Biol.* **2011**, *6*, 733–743.
- [31] a) S. Schneider, M. J. Gattner, M. Vrabel, V. Flugel, V. Lopez-Carrillo, S. Prill, T. Carell, *ChemBioChem* **2013**, *14*, 2114–2118; b) T. Yanagisawa, T. Sumida, R. Ishii, S. Yokoyama, *Acta Crystallogr. Sect. D* **2013**, *69*, 5–15; c) T. Yanagisawa, R. Ishii, R. Fukunaga, T. Kobayashi, K. Sakamoto, S. Yokoyama, *J. Mol. Biol.* **2008**, *378*, 634–652.
- [32] S. Bhaumik, S. S. Gambhir, *Proc. Natl. Acad. Sci. USA* **2002**, *99*, 377–382.
- [33] J. Zhao, S. Lin, Y. Huang, J. Zhao, P. R. Chen, *J. Am. Chem. Soc.* **2013**, *135*, 7410–7413.
- [34] a) A. M. Loening, T. D. Fenn, S. S. Gambhir, *J. Mol. Biol.* **2007**, *374*, 1017–1028; b) J. Woo, M. H. Howell, A. G. von Arnim, *Protein Sci.* **2008**, *17*, 725–735; c) A. M. Loening, T. D. Fenn, A. M. Wu, S. S. Gambhir, *Protein Eng. Des. Sel.* **2006**, *19*, 391–400.
- [35] a) Y. S. Wang, X. Fang, A. L. Wallace, B. Wu, W. R. Liu, *J. Am. Chem. Soc.* **2012**, *134*, 2950–2953; b) S. Greiss, J. W. Chin, *J. Am. Chem. Soc.* **2011**, *133*, 14196–14199.
- [36] D. Schwarzer, C. Ludwig, I. V. Thiel, H. D. Mootz, *Biochemistry* **2012**, *51*, 233–242.
- [37] a) O. Allnér, L. Nilsson, A. Villa, *J. Chem. Theory Comput.* **2012**, *8*, 1493–1502; b) K. L. Meagher, L. T. Redman, H. A. Carlson, *J. Comput. Chem.* **2003**, *24*, 1016–1025.
- [38] K. Lindorff-Larsen, S. Piana, K. Palmo, P. Maragakis, J. L. Klepeis, R. O. Dror, D. E. Shaw, *Proteins Struct. Funct. Bioinf.* **2010**, *78*, 1950–1958.
- [39] G. M. Morris, R. Huey, W. Lindstrom, M. F. Sanner, R. K. Belew, D. S. Goodsell, A. J. Olson, *J. Comput. Chem.* **2009**, *30*, 2785–2791.
- [40] T. A. Halgren, *J. Comput. Chem.* **1996**, *17*, 616–641.

Received: January 29, 2014

Published online on June 27, 2014